

Intense 1400-1600 nm circularly polarised luminescence from homo- and heteroleptic chiral erbium complexes

Oliver G. Willis,^a Andrea Pucci,^a Enrico Cavalli,^b Francesco Zinna ^{*a} and Lorenzo Di Bari ^{*a}

Compound preparation

The synthesis of CsEr(hfbc)₄ followed the literature procedure by Zinna et al.¹ The synthesis of [TMG-H⁺]₃Er(BINOLate)₃ followed a modified procedure by Walsh and co-workers² which has been published by Di Bari et al.³ The synthesis of each enantiomer of the complexes Er(NTA)₃⁻ⁱPrPyBox and Er(NTA)₃PhPyBox followed a modified procedure by Zinna and Di Bari.⁴ The reactions were performed under a N₂ atmosphere with reactants and solvents used as received from the supplier with no further purification. CHNS analyses were performed with a vario MICRO cube CHNOS Elemental Analyzer GmbH. Both CsEr(hfbc)₄ and [TMG-H⁺]₃Er(BINOLate)₃ have been previously fully characterized.³

Preparation of Er(NTA)₃·2H₂O

KOH (52 mg, 0.9 mmol) was dissolved in ethanol (2 mL) and added to a solution of 4,4,4-trifluoro-1-(2-naphthyl)-1,3-butanedione (NTA, 245 mg, 0.9 mmol) in ethanol (10 mL) under stirring. ErCl₃ hexahydrate (117 mg, 0.3 mmol) was dissolved in water (2 mL) and added dropwise to the reaction mixture. The solution was then refluxed under stirring for 4 hours. The solvent was removed under reduced pressure and the crude solid dissolved in dichloromethane (10 mL) and extracted three times with water (5 mL). The organic phase was dried under Na₂SO₄, and then filtered. The solvent removed under reduced pressure to yield the title compound as a yellow solid (257 mg, 86%) and used without any further purification.

Preparation of Er(NTA)₃(R,R)-⁻ⁱPrPyBox

Er(NTA)₃·H₂O (50 mg, 0.05 mmol) and (R,R)-⁻ⁱPrPyBox (15 mg, 0.05 mmol) were dissolved in ethanol (4 mL) and heated under stirring at 60 °C for 4 h. The solvent was removed under reduced pressure to give a crude solid. The solid was purified by dissolving in dichloromethane (5 mL) and adding petroleum ether (15 mL). The precipitate was collected by filtration and dried under vacuum to give Er(NTA)₃(R,R)-⁻ⁱPrPyBox as a white solid (39 mg, 62%). Found: C, 56.5; H, 3.75; N, 2.7. Calc. for C₅₉H₅₀ErF₉N₃O₈·0.25C₄H₁₀: C, 56.2; H, 4.1; N, 3.3.

Preparation of Er(NTA)₃(S,S)-⁻ⁱPrPyBox

The same procedure as for Er(NTA)₃(R,R)-⁻ⁱPrPyBox was followed to give Er(NTA)₃(S,S)-⁻ⁱPrPyBox (37 mg, 59%). Found: C, 55.7; H, 3.55; N, 3.7. Calc. for C₅₉H₅₀ErF₉N₃O₈: C, 55.9; H, 4.0; N, 3.3.

Preparation of Er(NTA)₃(R,R)-PhPyBox

Er(NTA)₃·H₂O (50 mg, 0.05 mmol) and (R,R)-PhPyBox (18 mg, 0.05 mmol) were dissolved in ethanol (4 mL) and heated under stirring at 60 °C for 4 h. The solvent was removed under reduced pressure to give a crude solid. The solid was purified by dissolving in dichloromethane (5 mL) and adding petroleum ether (15 mL). The precipitate was collected by filtration and dried under vacuum to give Er(NTA)₃(R,R)-PhPyBox as a white solid (47 mg, 71%). Found: C, 58.4; H, 3.7; N, 2.95. Calc. for C₆₅H₄₆ErF₉N₃O₈: C, 58.5; H, 3.5; N, 3.15.

Preparation of Er(NTA)₃(S,S)-PhPyBox

The same procedure as for Er(NTA)₃(R,R)-PhPyBox was followed to give Er(NTA)₃(S,S)-PhPyBox (50 mg, 75%). Found: C, 59.2; H, 3.95; N, 3.0. Calc. for C₆₅H₄₆ErF₉N₃O₈·0.5C₆H₁₄: C, 59.25; H, 3.9; N, 3.05.

Instrumentation

Lifetime measurements

Lifetime measurements were carried out using an Edinburgh FLS1000 spectrofluorometer equipped with a pulsed Xe lamp, a double excitation monochromator, a single emission monochromator and a N₂ cooled NIR extended photomultiplier. All the spectra were measured at room temperature in THF solutions ranging in concentrations from 0.1 to 1 mM and corrected for the spectral responsiveness of the setup. The decay time was evaluated after reconvolution of the experimental decay profile taking into account the Instrumental Response Function (IRF), using the routine implemented in the software of the spectrofluorometer.

Quantum yield measurements

Luminescence quantum yields (or External Quantum Efficiency, EQE, Q_x^L) were measured with a Horiba Jobin–Yvon Fluorolog®-3 spectrofluorometer equipped with a 450 W Xenon arc lamp, double-grating excitation, and single-grating emission monochromators and with a liquid nitrogen-cooled InGaAs detector. The EQE and Internal Quantum Efficiency (IQE, Q_{Er}^{Er}) were calculated using Eqs. 1 and 2 respectively. The fluorescence quantum yields were measured in THF relative to Yb(TTA)₃(H₂O)₂ ($Q_r^L = 0.35\%$ in toluene).⁵

$$Q_x^L = Q_r^L \cdot \frac{A_r(\lambda)}{D_r \cdot n_r^2} \cdot \frac{D_x \cdot n_x^2}{A_x(\lambda)} \quad \text{Equation S1}$$

$$Q_L^{Er} = \eta_{sens} \times Q_{Er}^{Er} = \eta_{sens} \times \tau_{obs} / \tau_{rad} \quad \text{Equation S2}$$

In the previous two equations, A is the absorbance at the excitation wavelength, n is the refractive index and D the luminescence integrated intensity. The indices r and x stand for reference and sample respectively. The absorption and excitation wavelengths for complexes CsEr(hfbc)₄, Er(NTA)₃PhPyBox and Er(NTA)₃PrPyBox was at 332 nm and at 365 nm for [TMG–H⁺]₃Er(BINOLate)₃. The observed lifetime is τ_{obs} and τ_{rad} is the radiative lifetime of the Ln(III). Finally, the efficiency of the ligand-to-erbium energy transfer process is given as η_{sens} .

UV-Vis/CD

UV-Vis spectra were recorded using a Jasco-V650 spectrophotometer in the spectral range of 200 to 600 nm. All samples were measured in THF with concentrations ranging from 0.6 to 3.2 mM at room temperature. The same solutions were used to record CD spectra using a J1500 spectropolarimeter in 0.01 cm optical glass cells and averaging from 1 to 16 accumulations.

NIR-CD/NIR-Abs

NIR-CD measurements were performed using a Jasco J200 spectropolarimeter provided with an ADC system. All complexes were measured in THF with concentrations ranging from 16 mM to 37 mM, depending on the complexes solubility, in 1 cm optical glass cells with parameters as follows: Scan speed 100 nm/min, slit width 2–4 nm, integration time 4 sec and accumulations from 3 to 8. The spectra were baseline corrected by subtraction of the solvent spectrum. The same solutions were used to measure the corresponding NIR absorption spectra using a Cary 5000 UV-Vis-NIR spectrophotometer.

NIR-CPL

Emission spectra were recorded using a Horiba Jobin–Yvon Fluorolog®-3 spectrofluorometer equipped with a 450 W Xenon arc lamp, double-grating excitation, and single-grating emission monochromators and with a liquid nitrogen-cooled InGaAs detector. Discrimination of left- and right-CP light was achieved using a quarter waveplate and linear polarizer, suitable within the 1400 to 1600 nm spectral region, from Edmund Optics. The optics were placed into custom 3D-printed holders (52 × 52 mm), which were placed between the sample and detector. Subsequent manual rotations of the QWP by 90° allowed for the measurements of the two states of polarization. The CPL ($I_L - I_R$) and total emission (average of I_L and I_R) were then extracted. Each fluorescence measurement utilized a 0.5 sec integration time over 201 points meaning each scan lasted ca. 1 min 40 sec. For CsEr(hfbc)₄, one full rotation with one acquired emission profile per position was measured. The Er(NTA)₃PhPyBox complex needed three full rotations and one spectrum per position, while [TMG–H⁺]₃Er(BINOLate)₃ needed one complete rotation with eight accumulations per positions. Overall, the total time for measuring the CPL ranged from ca. 6 minutes to one hour.



Figure S1. The 3D-printed holder for the QWP and LP, showing both the front view, each of the individual layers and finally the combined set-up.

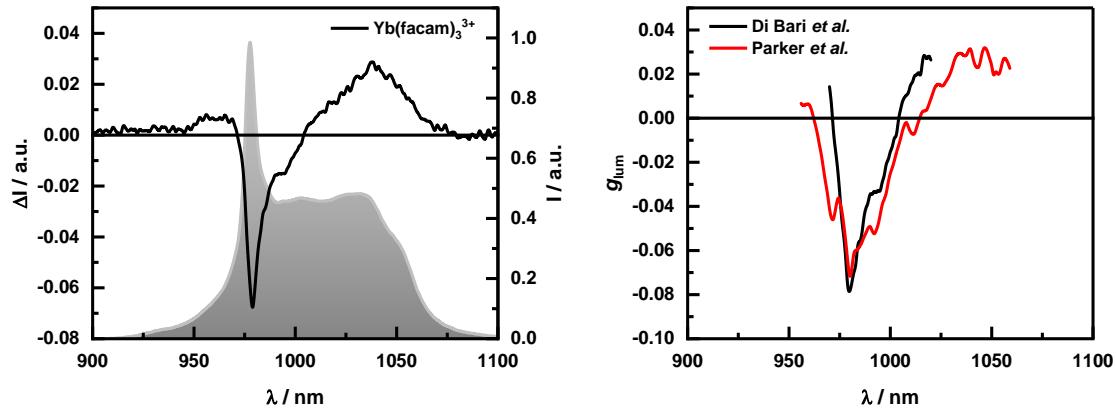


Figure S2. Left: The NIR-CPL spectrum of $\text{Yb}(\text{facam})_3^{3+}$ in DMSO with normalised average total emission traced in the background (in grey, $\lambda_{\text{ex}} = 325 \text{ nm}$). Right: The g_{lum} -vs-wavelength plot for $\text{Yb}(\text{facam})_3^{3+}$ measured in this work (Black) and by Parker⁶ (Red).

B_{CPL}

Given the complex structure of CPL spectra with several opposite bands within the same manifold, a more general definition of B_{CPL} factor was employed:

$$B_{\text{CPL}} = \varepsilon \cdot \phi \cdot \frac{1}{2} \frac{\int_{\lambda_a}^{\lambda_b} I(\lambda) g(\lambda) d\lambda}{\int_{\lambda_i}^{\lambda_f} I(\lambda) d\lambda} \quad \text{Equation S3}$$

Where the integral in the numerator has to be estimated between the extrema of the considered transition (λ_a , λ_b), while the integral in the denominator is calculated over the whole emission range (λ_i , λ_f). Note that if $g(\lambda)$ does not change sign within a term-to-term transition and it is approximately constant ($g(\lambda) \approx \bar{g}$), then the above definition is reduced to:

$$B_{\text{CPL}} = \varepsilon \cdot \phi \cdot \frac{1}{2} \bar{g} \cdot \frac{\int_{\lambda_a}^{\lambda_b} I(\lambda) d\lambda}{\int_{\lambda_i}^{\lambda_f} I(\lambda) d\lambda} = \varepsilon \cdot \phi \cdot \frac{1}{2} \bar{g} \cdot \beta \quad \text{Equation S4}$$

According to the usual definition applicable to lanthanide CPL.⁷

Additional spectra

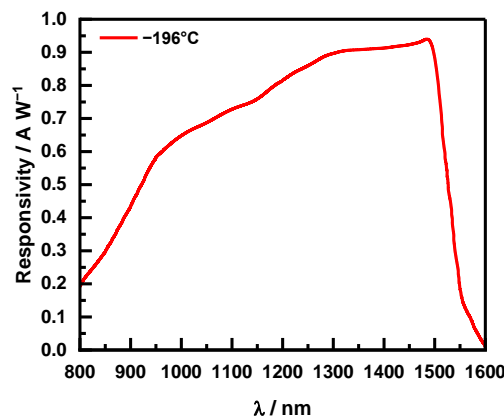


Figure S3. IGALN-series InGaAs photodiode typical spectral response recreated from the HORIBA scientific manual.

Spectra for $\text{CsEr}(\text{hfbc})_4$

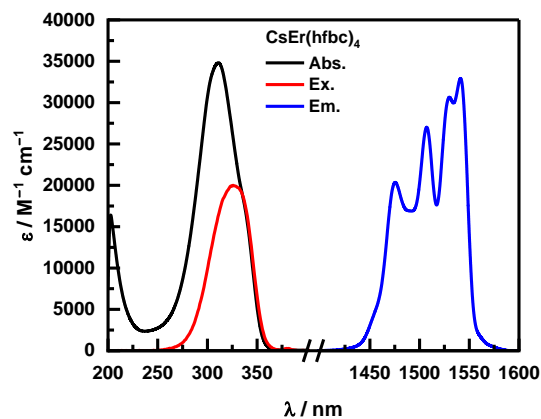


Figure S4. Absorption spectra of $\text{CsEr}(\text{hfbc})_4$ in black, with the excitation spectrum in red superimposed ($\lambda_{\text{em}} = 1542 \text{ nm}$). The emission spectrum is shown in blue ($\lambda_{\text{ex}} = 325 \text{ nm}$). All measurements were carried out in 0.1 mM anhydrous THF solutions at room temperature.

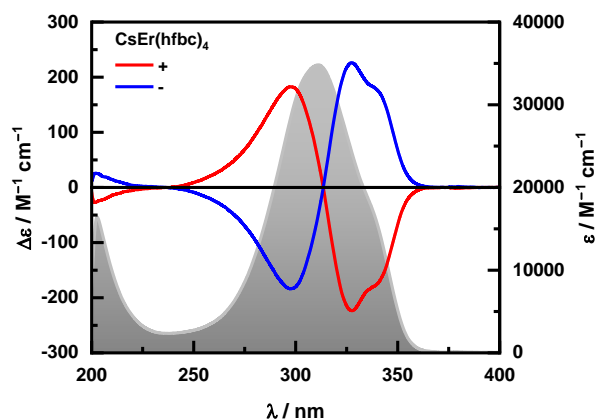


Figure S5. Electronic circular dichroism (ECD) spectra of the two enantiomers of the $\text{CsEr}(\text{hfbc})_4$ complex with total absorption traced in the background (in grey). All samples were measured in 3.2 mM THF solutions with a 0.01 cm path length at room temperature.

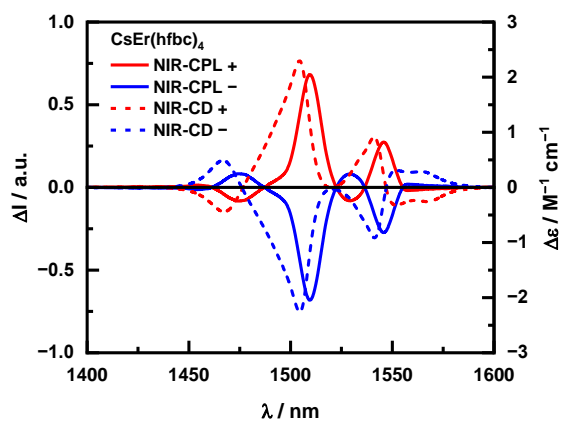


Figure S6. The NIR-CD (dashed lines) and NIR-CPL (solid lines) of the two enantiomers of $\text{CsEr}(\text{hfbc})_4$.

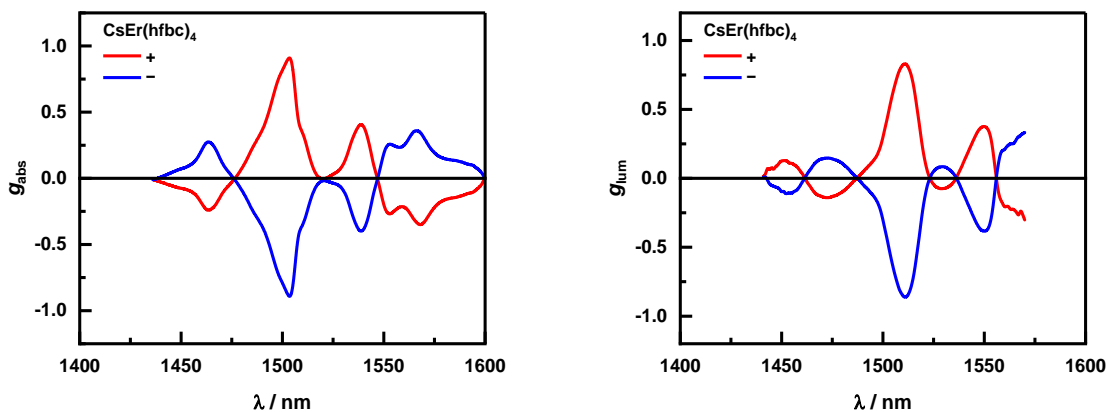


Figure S7. Left: The g_{abs} -vs-wavelength plot for each enantiomer of $\text{CsEr}(\text{hfbc})_4$. Right: The g_{lum} -vs-wavelength plot for each enantiomer of $\text{CsEr}(\text{hfbc})_4$.

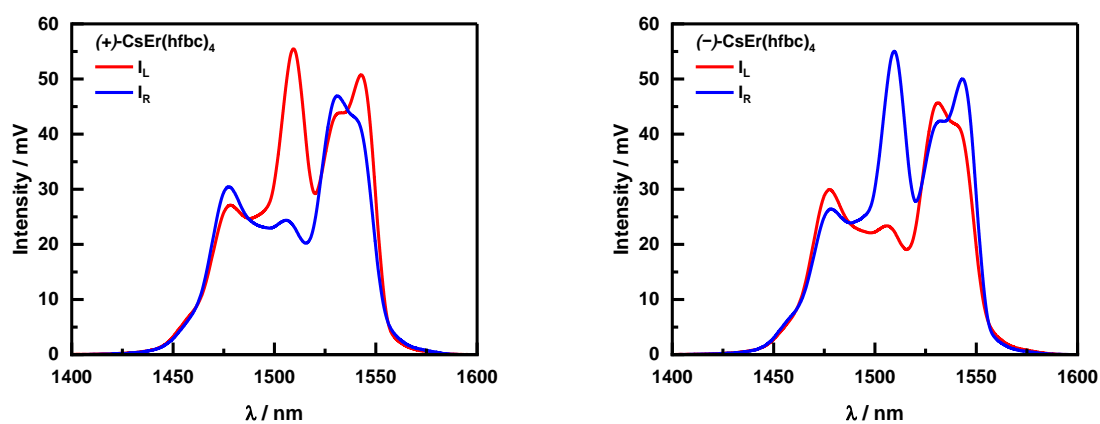


Figure S8. Total luminescence intensity of the two circularly polarized components, where I_L and I_R are the left- and right-components respectively. Left: The emission spectra of each polarization for (+)- $\text{CsEr}(\text{hfbc})_4$. Right: The emission spectra of each polarization for (-)- $\text{CsEr}(\text{hfbc})_4$.

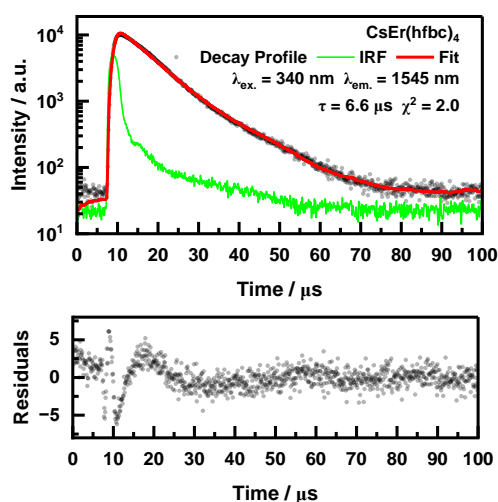


Figure S9. The $\text{CsEr}(\text{hfbc})_4$ decay curve of the $^4I_{13/2}$ excited state of Er^{3+} along with the reconvolution fitting. Measurements carried out in 0.1 mM THF solutions at room temperature.

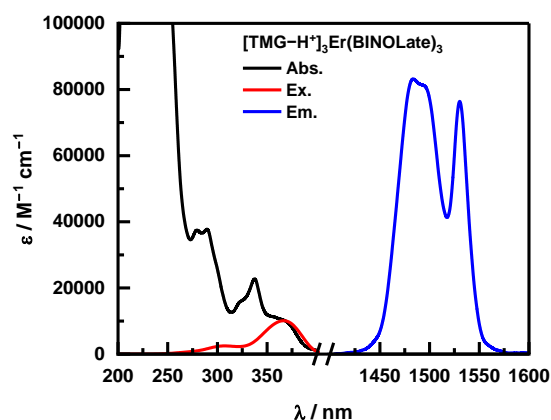
Spectra for $[\text{TMG-H}^+]_3\text{Er}(\text{BINOLate})_3$ 

Figure S10. Absorption spectra of $[\text{TMG-H}^+]_3\text{Er}(\text{BINOLate})_3$ in black, with the excitation spectrum in red superimposed ($\lambda_{\text{em}} = 1485 \text{ nm}$). The emission spectrum is shown in blue ($\lambda_{\text{ex}} = 365 \text{ nm}$). All measurements were carried out in 1 mM anhydrous THF solutions at room temperature.

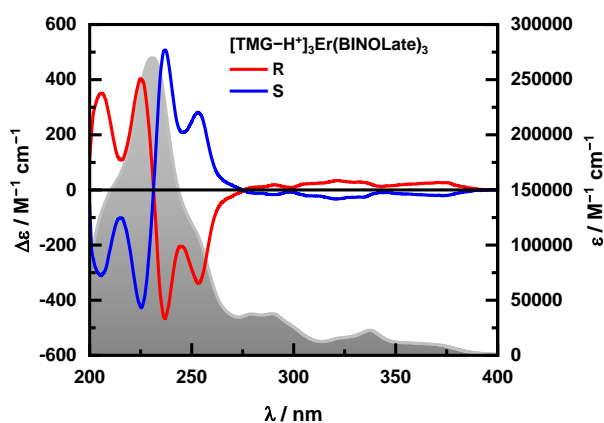


Figure S11. Electronic circular dichroism (ECD) spectra of the two enantiomers of the $[\text{TMG-H}^+]_3\text{Er}(\text{BINOLate})_3$ complex with total absorption traced in the background (in grey). All samples were measured in 0.6 mM anhydrous THF solutions with a 0.01 cm path length at room temperature.

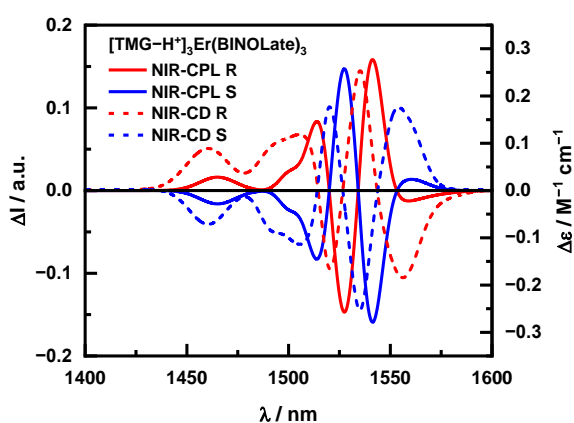


Figure S12. The NIR-CD (dashed lines) and NIR-CPL (solid lines) of the two enantiomers of $[\text{TMG-H}^+]_3\text{Er}(\text{BINOLate})_3$.

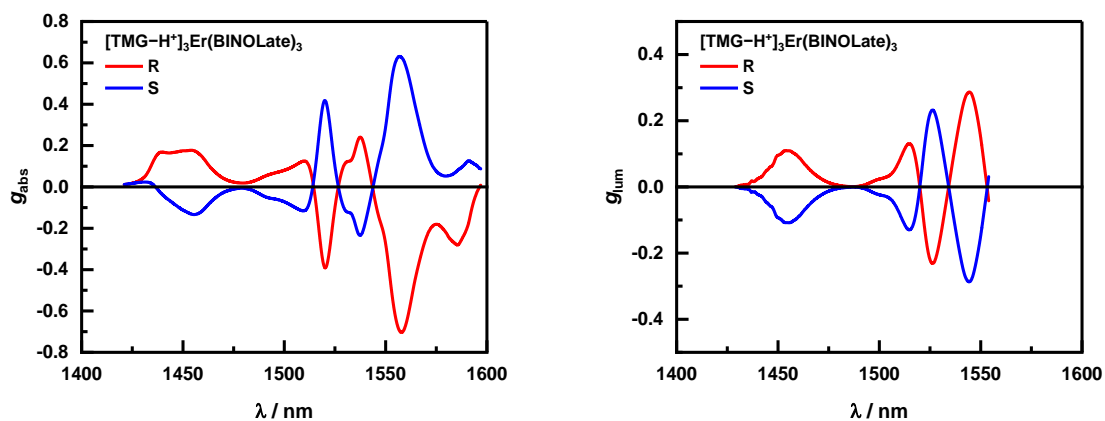


Figure S13. Left: The g_{abs} -vs-wavelength plot for each enantiomer of $[\text{TMG-H}^+]_3\text{Er}(\text{BINOLate})_3$. Right: The g_{lum} -vs-wavelength plot for each enantiomer of $[\text{TMG-H}^+]_3\text{Er}(\text{BINOLate})_3$.

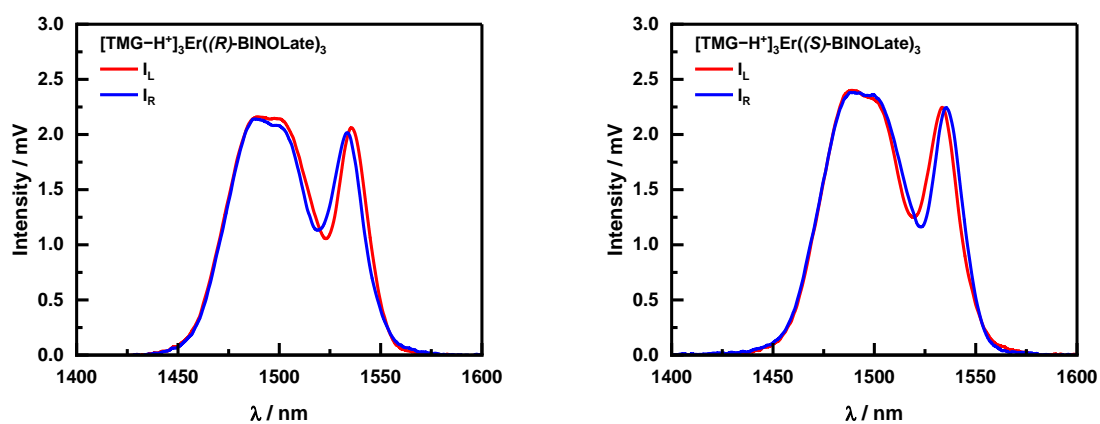


Figure S14. Total luminescence intensity of the two circularly polarized components, where I_L and I_R are the left- and right-components respectively. Left: The emission spectra of each polarization for $[\text{TMG-H}^+]_3\text{Er}((R)\text{-BINOLate})_3$. Right: The emission spectra of each polarization for $[\text{TMG-H}^+]_3\text{Er}((S)\text{-BINOLate})_3$.

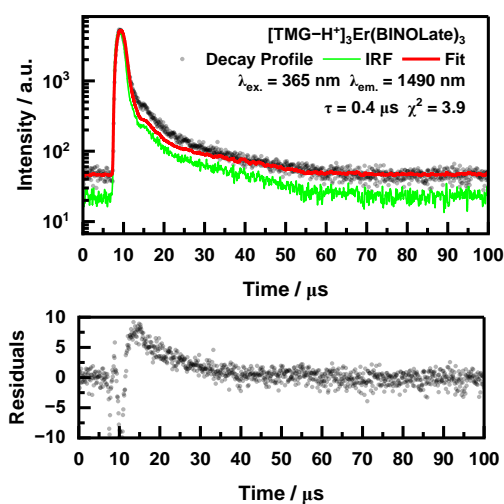


Figure S15. The $[\text{TMG-H}^+]_3\text{Er}(\text{BINOLate})_3$ decay curve of the ${}^4I_{13/2}$ excited state of Er^{3+} along with the reconvolution fitting. Measurements carried out in 1 mM THF solutions at room temperature.

Spectra for $\text{Er}(\text{NTA})_3\text{PhPyBox}$

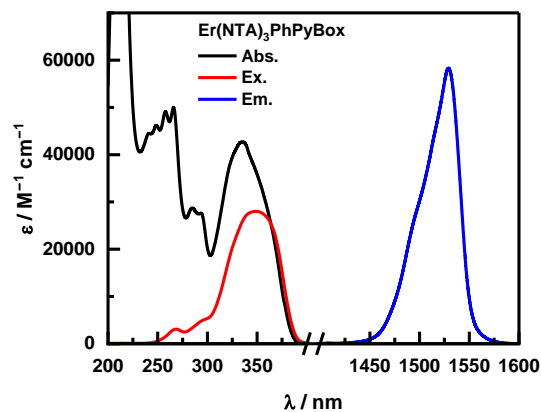


Figure S16. Absorption spectra of $\text{Er}(\text{NTA})_3\text{PhPyBox}$ in black, with the excitation spectrum in red superimposed ($\lambda_{\text{em}} = 1530$ nm). The emission spectrum is shown in blue ($\lambda_{\text{ex}} = 345$ nm). All measurements were carried out in 0.1 mM anhydrous THF solutions at room temperature.

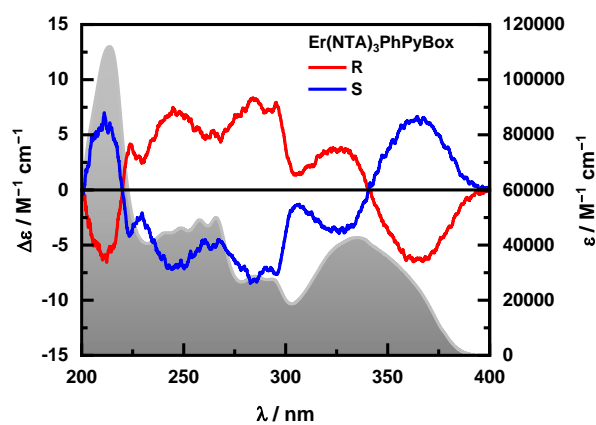


Figure S17. Electronic circular dichroism (ECD) spectra of the two enantiomers of the $\text{Er}(\text{NTA})_3\text{PhPyBox}$ complex with total absorption traced in the background (in grey). All samples were measured in 1 mM anhydrous THF solutions with a 0.01 cm path length at room temperature.

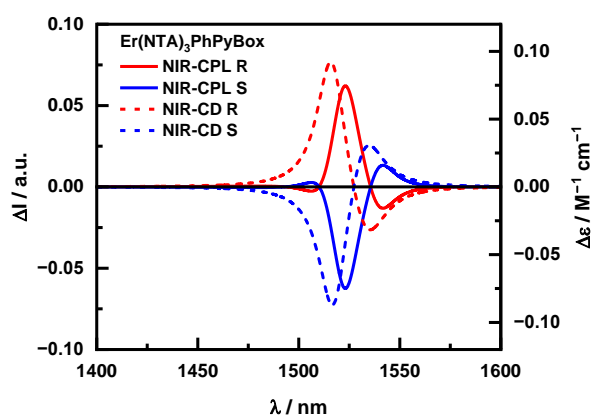


Figure S18. The NIR-CD (dashed lines) and NIR-CPL (solid lines) of the two enantiomers of $\text{Er}(\text{NTA})_3\text{PhPyBox}$.

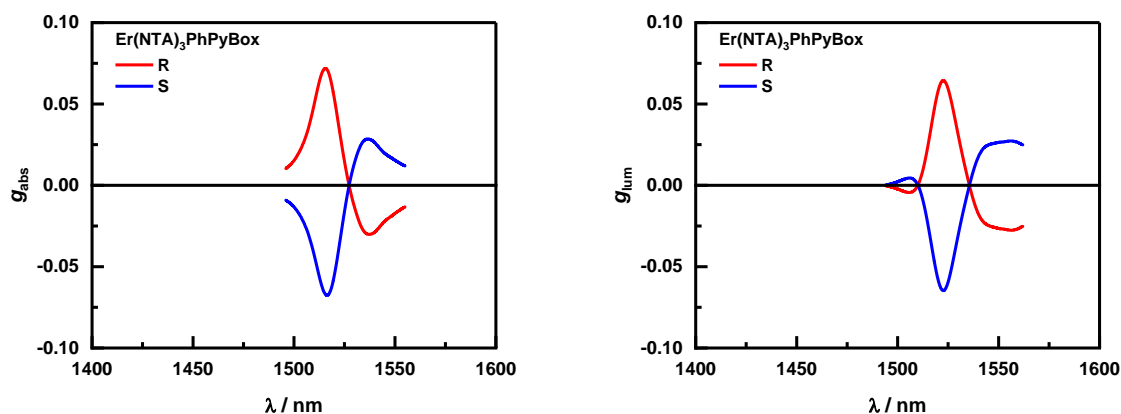


Figure S19. Left: The g_{abs} -vs-wavelength plot for each enantiomer of $\text{Er}(\text{NTA})_3\text{PhPyBox}$. Right: The g_{lum} -vs-wavelength plot for each enantiomer of $\text{Er}(\text{NTA})_3\text{PhPyBox}$.

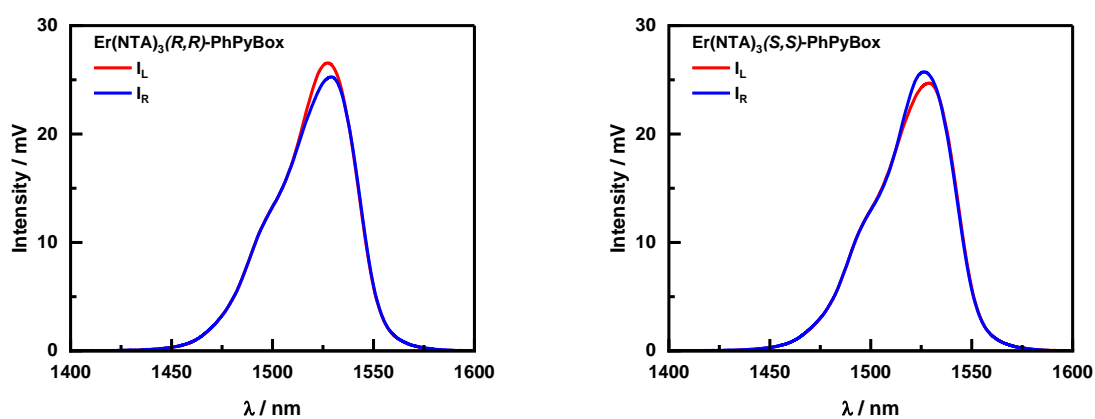


Figure S20. Total luminescence intensity of the two circularly polarized components, where I_L and I_R are the left- and right-components respectively. Left: The emission spectra of each polarization for $\text{Er}(\text{NTA})_3(\text{R,R})\text{-PhPyBox}$. Right: The emission spectra of each polarization for $\text{Er}(\text{NTA})_3(\text{S,S})\text{-PhPyBox}$.

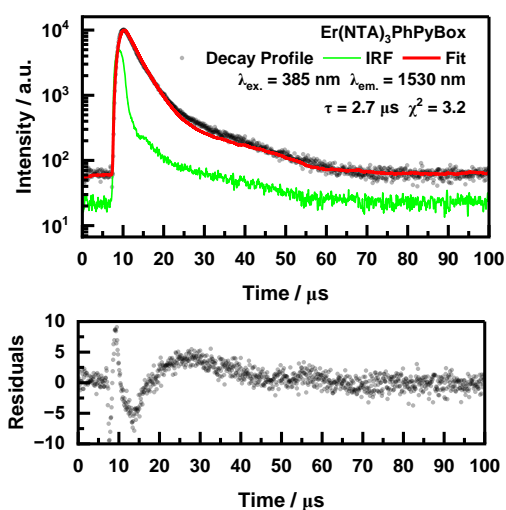


Figure S21. The $\text{Er}(\text{NTA})_3\text{PhPyBox}$ decay curve of the $^4I_{13/2}$ excited state of Er^{3+} along with the reconvolution fitting. Measurements carried out in 1 mM THF solutions at room temperature.

$\text{Er}(\text{NTA})_3\text{iPrPyBox}$

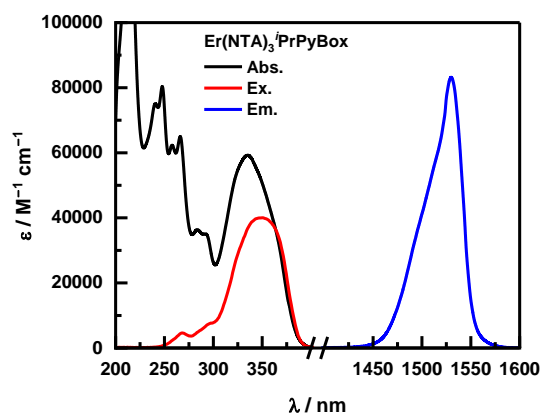


Figure S22. Absorption spectra of $\text{Er}(\text{NTA})_3\text{PrPyBox}$ in black, with the excitation spectrum in red superimposed ($\lambda_{\text{em}} = 1530$ nm). The emission spectrum is shown in blue ($\lambda_{\text{ex}} = 345$ nm). All measurements were carried out in 0.1 mM anhydrous THF solutions at room temperature.

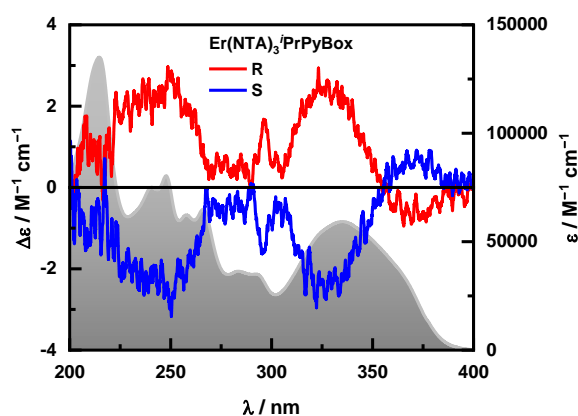


Figure S23. Electronic circular dichroism (ECD) spectra of the two enantiomers of the $\text{Er}(\text{NTA})_3\text{PrPyBox}$ complex with total absorption traced in the background in grey). All samples were measured in 0.9 mM anhydrous THF solutions with a 0.01 cm path length at room temperature.

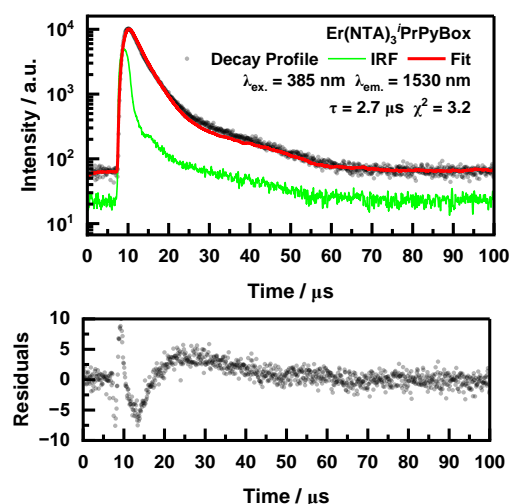


Figure S24. The $\text{Er}(\text{NTA})_3\text{PrPyBox}$ decay curve of the $^4I_{13/2}$ excited state of Er^{3+} along with the reconvolution fitting. Measurements carried out in 1 mM THF solutions at room temperature.

Notes and references

- 1 F. Zinna, U. Giovanella and L. Di Bari, *Adv. Mater.*, 2015, **27**, 1791–1795.
- 2 J. R. Robinson, X. Fan, J. Yadav, P. J. Carroll, A. J. Wooten, M. A. Pericàs, E. J. Schelter and P. J. Walsh, *J. Am. Chem. Soc.*, 2014, **136**, 8034–8041.
- 3 O. G. Willis, F. Zinna, G. Pescitelli, C. Micheletti and L. Di Bari, *Dalton Trans.*, 2022, **51**, 518–523.
- 4 F. Zinna, L. Arrico and L. Di Bari, *Chem. Commun.*, 2019, **55**, 6607–6609.
- 5 S. Meshkova, Z. Topilova, D. Bolshoy, S. Belyukova, M. Tsvirko and V. Venchikov, *Acta Phys. Pol. A*, 1999, **95**, 983–990.
- 6 C. L. Maupin, R. S. Dickins, L. G. Govenlock, C. E. Mathieu, D. Parker, J. A. G. Williams and J. P. Riehl, *J. Phys. Chem. A*, 2000, **104**, 6709–6717.
- 7 L. Arrico, L. Di Bari and F. Zinna, *Chem. – Eur. J.*, 2021, **27**, 2920–2934.